# Design of Microstrip antenna by Integrating Octagonal Patch Configuration for UWB Application

**Sonal Patil, and Ashwini Naik**
Department of Electronics and Telecommunication Engineering, Ramrao Adik Institute of Technology, Navi Mumbai, Maharashtra, India.

Corresponding author: e-mail: sonalpatil606a@gmail.com

**ABSTRACT** This work proposes gain enhancement of the microstrip antenna to use in applications operated in UWB spectrum. The antenna structure comprises integrated octagonal shaped radiator and slotted ground plane fabricated on easily available FR4 substrate. The 50 Ω microstrip line fed octagonal shaped microstrip antenna is simulated by using Ansys high-frequency structure simulator. The radiator is modified by integrating patch configuration to achieve gain improvement. The modified antenna is modelled by vertically integrating two octagonal shaped patches, etching off small two square slots and small square slot of dimension 1 mm × 1 mm positioned at the mid width of the ground. The designed MI-OMSA structure is fabricated on double sided copper flame retardant epoxy glass composite dielectric substrate having size of 37 mm × 40 mm and tested by using vector network analyzer. The optimized MI-OMSA structure provides minimum return loss characteristically below -10 dB over 2.42 – 11.72 GHz frequency range, covering bandwidth of 9.31 GHz. The peak gain observed at 8.2 GHz is 6.7 dB. The structure demonstrates constant group delay over the operating spectrum. An ultra-wideband performance is achieved as antenna resonates at four frequencies. The antenna structure offers radiation pattern of omnidirectional and hence most fit for use in UWB applications. An UWB application, breast cancer detection is tested using proposed structure.

**INDEX TERMS** MSA, OMSA, MI-OMSA, Radiator, UWB, Breast Cancer Detection.

## I. INTRODUCTION

THE key component of wireless technology is antenna. The technology for wireless communication has developed rapidly, and compliance with the standards has to led an increase in the demand of antennas covering wide frequency range with higher gain. The omnipresence of wireless communication promotes the research on wide range of antennas incorporating various shapes and numerous sizes making them suitable for different applications. The antennas with omnidirectional radiation pattern are best fit for the applications in the short-range communication systems. This constrained requirement of reduced size, lower development cost, increased functionality, better performance and electrical parameters of antenna has increased the demand and usage of microstrip antenna (MSA). These antennas are prevalent as they offer numerous benefits such as small size, planar structure, low profile, less cumbersome, cost effective, easily fabricate and integrate with MMICs. Microstrip patch antennas have broad applications in wireless communication system.

Federal Communication Commission (FCC) has officially granted permission to the measurement procedures for emission from the devices to operate in the frequency spectrum ranging from 3.1 GHz to 10.6 GHz. This unlicensed ultra-wideband is enticing and can be utilized for medical and communication applications because it offers wide operating frequency band, consumes less power, higher transmission data rates, greater reliability [1]. The design considerations of printed monopole antennas for different radiating patch shape configurations for UWB technology have been reported in [2]. For UWB applications, the radiating patch was studied in conjunction with slots, with and without asymmetrical U-shaped and T-shaped slots, similarly shaped to the patch and ground slot. Although combinations were intended to achieve dual circular polarization and wide bandwidth, the structures produce reduced gain and an unstable radiation pattern [3-5]. The radiation characteristics of the printed circular antenna with FR4, duroid, and foam type dielectric material were examined. The better omnidirectional radiation performance was observed when the substrate's thickness reduced with a low dielectric constant, but the cross-polar component significantly deteriorated [6]. UWB antennas of rectangular patch with diamond shaped slot, proximity-fed circular shaped disk with an open ring and π-shaped slot, two octagonal patch configurations with circular slot and two quarter elliptical slots in the ground section, dodecagon shaped patch and self-complementary square monopole

antenna with defected ground were designed for bandwidth enhancement. To preserve the radiation properties, the slots were etched off at the areas having less current distribution [7-11]. The pentagon rings, square ring patches, fusion of rectangular antennas with I-shaped patches and two C-type slot sections, slotted rectangular radiators with tapered slots at the ground plane, and rectangular-shaped inset-fed MSA were discovered as low-cost and compact UWB antennas. The gain offered by these structures ranges from 2.45 to 5.76 dB [12–16]. The 4 × 1 MIMO antennas with elliptical patch designed on Rogers 5880 substrate to operate in ultra-wideband range, provides 5.9 dB maximum gain were reported in [17]. Gain enhancement were achieved by designing the structure with parasitic resonator, circular resonator, circular slotted radiator with defected ground and an elliptical shaped radiator with two U-shaped inverted slots. The gain of these structures ranged from -1.98 to 5.8 dB, and they were designed for on-body communication and microwave imaging [18-21]. The antennas for UWB applications, especially for wireless communication and tri-band applications, were designed with quarter circular geometry and inverted L-shaped radiator, octagonal MSA by stepping rectangular MSA, a circular ring-shaped radiator with small circles between two circular rings. The antenna design becomes more complex with this kind of geometry [22-24]. The innovative antennas of U-shaped slots in radiator for breast cancer detection and hard surface H-resonator arrays for stable radiation pattern, combination of single split ring resonator and circular complementary split-ring resonator for band rejection properties, different substrate materials suitable for the human body surface were analyzed. The reconfigurable metamaterial antenna and multi-mode pattern MSA configuration based on electromagnetic ground defects for contemporary wireless communication devices provided the steady gain and gain-bandwidth enhancement; despite this, the structures are large in size and intricate [26-29].

The conventional rectangular and circular patch antennas are designed to operate in UWB spectrum and observed that the structure resonates effectively at a single resonance frequency, but has less bandwidth. Due to these noted limitations, this antenna is inadequate for use in contemporary communication systems in its current configuration. In perspective of these constraints, this antenna is progressively modified to an octagonal configuration. The proposed work focuses on designing a line fed MSA with a unified octagonal radiating patch configuration which can be suitable for breast cancer detection. The research on microwave sensing has grown exponentially, with multiple radiating elements leading to complex and bulky systems. Also, the single antenna sensor with single feed point is proposed to reduce size, complexity and cost compared to devices having multiple radiating elements. The antenna sensor offering an omnidirectional radiation pattern, can help in improving the sensor's sensitivity. The system sensing capability can be improved by designing an efficient UWB antenna sensor with high gain and stable radiation pattern to scan dense area. The UWB antennas are more attractive as they will have wide frequency band and ability to generate multiple resonance frequencies. These multiple resonances are beneficial for better insights in the dense part of the object. The five sections of the paper are prepared to describe this work. The second section of this paper describes antenna geometry and design theory details. The results are discussed in the third section. The fourth section compares proposed work with the literature. Finally, this work is concluded in the fifth section.

## II. ANTENNA GEOMTRY AND DESIGN THEORY

### A. ANTENNA GEOMETRY

The microstrip patch antenna of simple octagonal shape (SOMSA) is designed by using FR-4 epoxy material having dielectric properties as 1.59 mm thick substrate, $\varepsilon_r$ of 4.4 and tan δ of 0.02. The electromagnetic waves generated through radiating element fringe off patch into the substrate. These waves radiate into the air after being reflected from the ground plane. The fringing field between the patch and ground causes the radiations to occur. The technique to construct a regular octagon is as a quasiregular truncated square with two distinct kinds of edges alternately. The one way to design the symmetrical shape is octagon inscribed with a square and square dimensions can be found using mentioned formulae. As a consequence, the structure is initially designed by referring rectangular microstrip antenna with following formulae.

For $W/h > 1$,

$$W=\frac{\lambda_o}{2\sqrt{\frac{\varepsilon_r+1}{2}}} \quad (1)$$

$$\varepsilon_{re}=\frac{\varepsilon_r+1}{2}+\frac{\frac{\varepsilon_r-1}{2}}{\sqrt{1+\frac{12h}{W}}} \quad (2)$$

$$\Delta L=0.412\,h\,\frac{(\varepsilon_{re}+0.3)\left(\frac{W}{h}+0.264\right)}{(\varepsilon_{re}-0.258)\left(\frac{W}{h}+0.8\right)} \quad (3)$$

$$L=\frac{\lambda_o}{2\sqrt{\varepsilon_{re}}}-2\Delta L \quad (4)$$

where, $W$: width of the patch, $\varepsilon_r$: dielectric constant, $\varepsilon_{re}$: effective dielectric constant, $\lambda_o$: free space wavelength, $\Delta L$: the effective length, $h$: the thickness of the dielectric substrate, $L$: length of the patch.

The antenna structure is designed to operate in the spectrum of UWB covering span of 3.1 – 10.6 GHz. The operating frequency of 6.85 GHz and wavelength of 43.796 mm are used to calculate the dimensions of the rectangular patch. The antenna structure is designed with patch length of 9.806 mm and patch width of 13.32 mm to obtain minimum return loss. These electrical dimensions of the patch are used to design the length (L) and width (W) of the radiating patch having convex octagon shape as represented in fig. 1 (ii). The octagonal

shaped patch antenna is optimized with the electrical dimensions of 14 mm × 14 mm to exhibit good reflection characteristics. The substrate dimensions chosen to build the structure are of three times of the patch dimensions. The octagonal microstrip patch antenna (OMSA) structure is modelled using Ansys HFSS software.

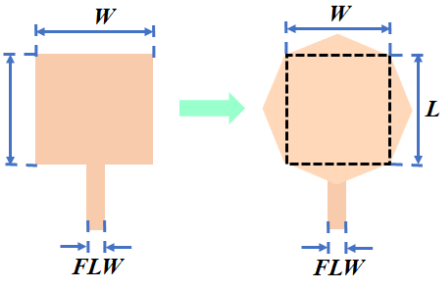


**FIGURE. 1:** Geometry of Rectangular and Octagonal MSA

### *B. INTEGRATED OMSA DESIGN*

The study been conducted for gain enhancement by integrating radiating patches. The radiating patch of octagonal configuration is modified by unifying two octagonal shaped patches to increase the conduction area as a result increase in the surface current that translates into a higher gain. As the conduction area is increased fringing field between radiator and patch increases thereby more radiations occur. When generated electromagnetic waves are in-phase, constructive interference created which results in the gain enhancement.

#### 1) HORIZONTALLY-INTEGRATED OMSA

The horizontally integrated octagonal microstrip antenna (HI-OMSA) is designed by integrating two octagonal shaped patches horizontally at the vertex.

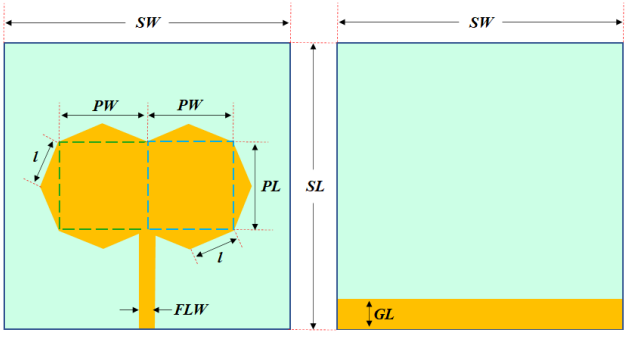


**FIGURE. 2:** Geometry of Horizontally Integrated OMSA

The antenna is designed with a patch width (*PW*) of 10 mm, patch length (*PL*) of 10 mm, and an octagonal side length (*l*) of 9 mm, fabricated on an FR-4 dielectric substrate. The substrate of FR-4 epoxy material is having dielectric properties as 1.59 mm thick substrate, $\varepsilon_r$ of 4.4 and tan δ of 0.02. The partial ground plane of dimensions 40 mm × 12 mm (*GL* × *GW*) is designed on other side of the substrate layer. This structure is fed at the vertex by a microstrip line of 50 Ω having 3 mm width (*FLW*). The antenna geometry and design details are presented in fig. 1 and Table 1 respectively. The fig. 2 (i) shows the radiating patch and fig. 2 (ii) shows the geometry of ground plane. The antenna structure is optimized to provide minimum return loss and VSWR over ultra-wideband frequency range. The gain variations are depicted in fig. 13. The structure provides 4.9 dB peak gain at 8.2 GHz.

#### 2) VERTICALLY-INTEGRATED OMSA

The vertically integrated octagonal microstrip antenna (VI-OMSA) is modelled by unifying two octagonal patches vertically at the vertex. Each patch is having dimensions of 14 mm × 14 mm (*PL* × *PW*) with side length (*l*) of 8.2 mm. The antenna structure is optimized to obtain minimum return loss and VSWR over the UWB spectrum. The configuration of VI-OMSA is represented in fig. 3 and design details are listed in Table 1. The negative gain for HI-OMSA and VI-OMSA is observed at the lower frequencies.

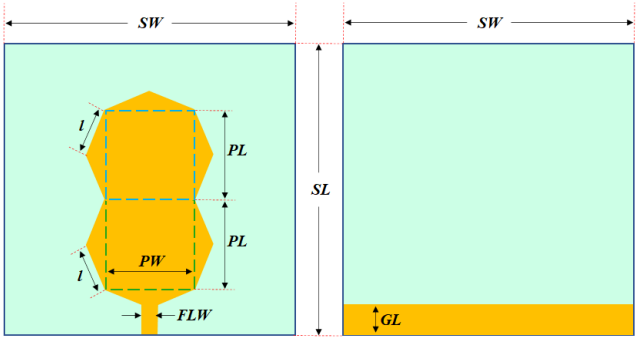


**FIGURE.3:** Geometry of Vertically Integrated OMSA

#### 3) MODIFIED-INTEGRATED OMSA

The gain improvement is obtained by inserting a small slot of 1 mm × 1 mm (*S3PL* × *S3PW*) dimension in the ground at the center of the substrate and two slots of 2 mm × 2 mm (*S1PL* × *S1PW and S2PL* × *S2PW*) dimensions in the radiating patch at the center of each integrated patch.

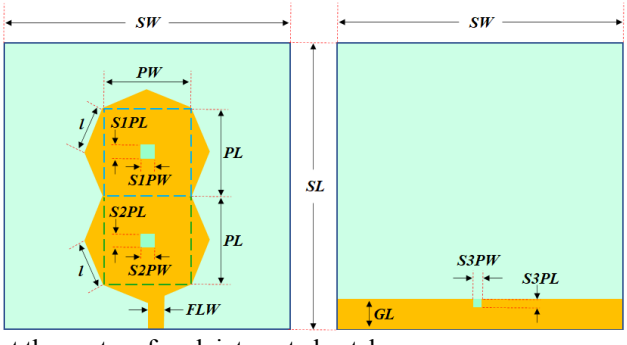


**FIGURE. 4:** Geometry of Modified Integrated OMSA

The geometry of the modified structure is represented in fig. 4 and design details are listed in Table 1. The antenna resonates in the fundamental mode over the lower band, while it resonates in the higher order modes over the upper band. The MI- OMSA is resonates at four frequencies, 3.45, 6.675, 8.2 and 10.67 GHz. These frequencies are presented as a parallel RLC circuit to form an electrical equivalent circuit of the MI-OMSA. The electrical equivalent circuit for the modified OMSA is depicted in fig. 5. The circuit element values are evaluated by using following formulae [25].

$$C = \frac{\varepsilon_o\, \varepsilon_{eff}\, L\, W}{2\, h \left[cos^2\left(\frac{\pi\, FP}{L}\right)\right]} \quad (5)$$

$$L = \frac{1}{\omega_r^2\, C} \quad (6)$$

$$R = \frac{Q_r}{\omega_r\, C} \quad (7)$$

$$Q_r = \frac{c\sqrt{\varepsilon_{eff}}}{4 f_r\, h} \quad (8)$$

where, $C$: Capacitance, $L$: Inductance, $R$: Resistance of parallel RLC equivalent circuit, $\varepsilon_{eff}$: effective permittivity of the medium, $\omega_r$: angular frequency, $W$: Patch Width, $h$: Substrate Thickness.

The 50 Ω feed line of 2 mm width and 3 mm length is represented by series combination of inductor ($L_f$) and capacitor ($C_f$) of value 0.11257 fH and 0.147 pF. A 50 Ω port is connected at the end for the excitation of antenna. Two square slots are placed in the double combined octets shaped antenna at the right optimized location of edge dimension 2 mm and a slot of size 1 mm × 1 mm in the reduced ground plane structure that may significantly makes the gain positive and negligible disturbances in the four resonating frequencies. Two square shape slots introduce the capacitive effects in the radiating patch and they represented as the parallel combination of $C_{s1}$ and $C_{s2}$. Each capacitance has the value 0.098 pF. The equivalent slot capacitance is represented as $C_S$ in the fig 5. The slit in ground plane is introduces negligible inductive effect but improves the MI-OSMA gain value. As the MI-OSMA is an UWB monopole antenna and resonates at four frequencies 3.45, 6.675, 8.2 and 10.67 GHz below -10 dB reflection coefficients value. Hence the antenna has quad tuned ultra-wideband behavior. These four resonance circuits are represented by four separate RLC parallel resonance circuits. The evaluated values of all passive elements are indicated on the circuit parameters using fundamental parallel resonance and microstrip discontinuities concepts [25]. An Ultra-wideband (UWB) performance from 2.42 GHz to 11.72 GHz is achieved by series combination of four parallel resonance circuits.

## III. RESULTS AND DISCUSSION

The HI-OMSA, VI-OMSA and MI-OMSA antenna structures are designed, optimized and simulated by using Ansys high-frequency structure simulator 2023 R2 software.

### *A. OPTIMIZATION FRAMEWORK*

#### 1) EFFECT OF SLOTS ($S_1$, $S_2$, $S_3$)

The MI-OMSA is modelled by etching off three slots, two ($S_1$ and $S_2$) in radiating patch and one ($S_3$) in ground plane as depicted in fig. 3. The upper slot $S_1$ and lower slot $S_2$ of dimension 2 mm × 2 mm in the radiating patch introduces capacitive effect while slot in ground $S_3$ of 1 mm × 1 mm size introduces inductive effect. The combination of $S_1$, $S_2$ and $S_3$ helps in optimizing the antenna structure by improving the return loss as presented in fig. 6.

#### 2) EFFECT OF RADIATING PATCH DIMENSIONS

The radiating patch is formed by integrating two octagonal patches. The length of the MI-OMSA structure is varied from 24, 26, 28, 30, 32 mm and width from 12, 13, 14, 15, 16 mm. It is observed that with increase in patch dimensions (15, 16 mm) and with decrease in patch dimensions (12, 13 mm), the return loss degrades at upper UWB and lower UWB respectively. The optimized square patch dimension of OMSA is 14 mm × 14 mm, exhibiting good reflection characteristics as presented in fig. 7.

**TABLE I.** Design Dimension Details of different OMSA

| Parameters | Description | Dimension (mm) | | |
|---|---|---|---|---|
| | | HI-OMSA | VI-OMSA | MI-OMSA |
| SW | Width of the substrate | 40 | 40 | 37 |
| SL | Length of the substrate | 40 | 40 | 40 |
| GW | Width of the ground plane | 40 | 40 | 37 |
| GL | Length of the ground plane | 12 | 3.5 | 3.5 |
| PW | Width of the radiating patch | 10 | 14 | 14 |
| PL | Length of the radiating patch | 10 | 14 | 14 |
| FLW | Width of the feedline | 3 | 2 | 2 |
| S1PW | Width of the first slot in radiating patch | - | - | 2 |
| S1PL | Length of the first slot in radiating patch | - | - | 2 |
| S2PW | Width of the second slot in radiating patch | - | - | 2 |
| S2PL | Length of the second slot in radiating patch | - | - | 2 |
| S3PW | Width of the ground slot | - | - | 1 |
| S3PL | Length of the ground slot | - | - | 1 |

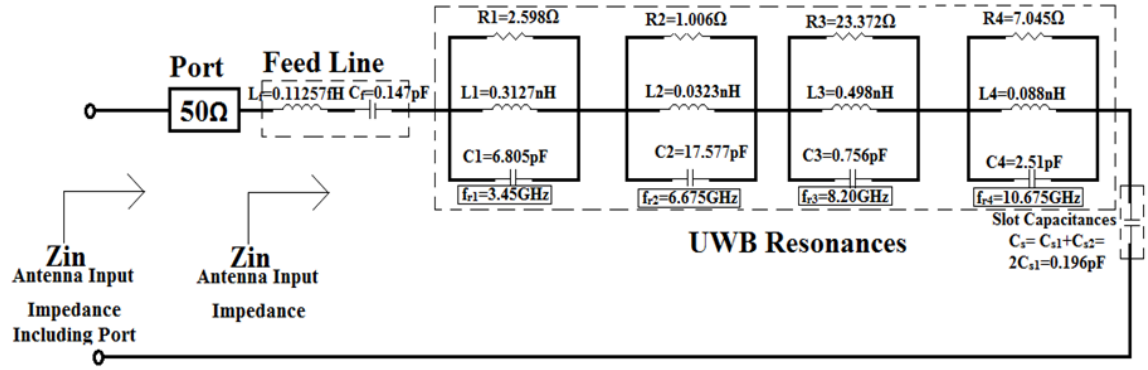


**FIGURE. 5:** Electric Equivalent details of MI-OMSA

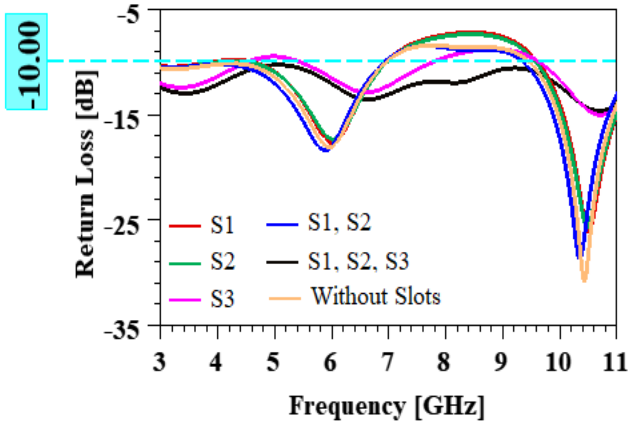


**FIGURE. 6:** Return Loss for different slot configurations (mm)

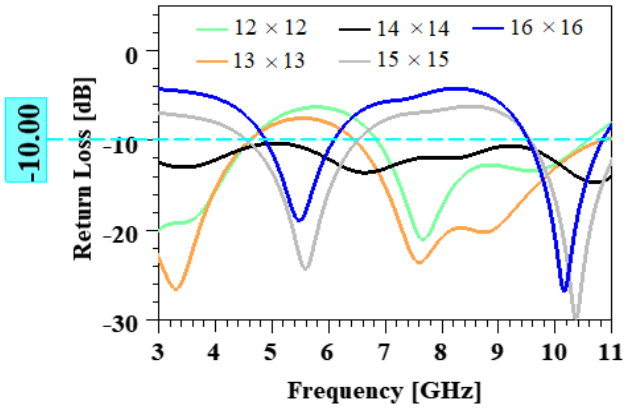


**FIGURE. 7:** Return Loss for different radiating patch dimensions (mm)

### 3) EFFECT OF SLOTS IN THE RADIATING PATCH

The two smaller slots (S1 & S2) are etched off from the radiating patch. The patch dimensions are varied from 1 mm × 1 mm to 3 mm × 3 mm with step size of 0.5 mm to optimize the antenna structure. The decrease in slot dimension, increases inductive effect and degrades the return loss as presented in fig. 8. The optimized S1 and S2 dimensions are 2 mm × 2 mm.

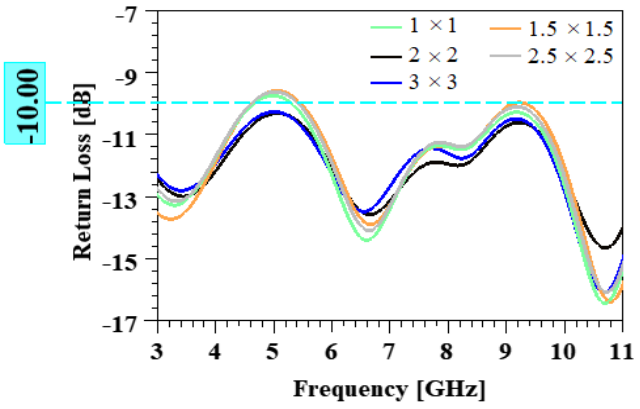


**FIGURE. 8:** Return Loss for slots (S1PD & S2PD) in radiating patch of different dimensions (mm)

### 4) EFFECT OF SLOT IN THE GROUND PLANE

A small slit ($S_3$) is etched off from the ground surface of size 1 mm × 1 mm. This slot introduces capacitive effect. The incorporation of $S_1$, $S_2$ and $S_3$ is found beneficial to improve the reflection characteristics. The antenna structure is optimized to obtain minimum return loss by varying width of $S_3$ from 0.5 to 4 mm as shown in fig. 9. It is observed that with increase in the slot width $S_{11}$ degrades.

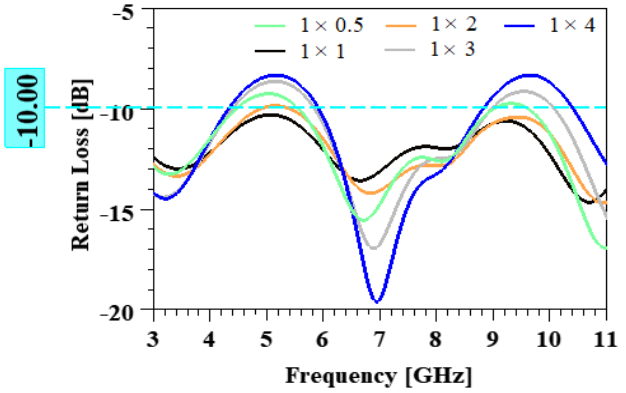


**FIGURE. 9:** Return Loss for slot (S3PD) in ground plane of different dimensions (mm)

5) EFFECT OF PARTIAL GROUND PLANE

The MI-OMSA antenna structure is optimized to investigate the effect of partial ground surface. The structure is optimized for different ground dimensions as presented in fig. 10. The ground plane length is varied for the dimensions of 40, 20, 10, 5 and 3.5 mm with width of 37 mm. The partial ground plane is advantageous to improve the antenna performance. The reduction in the ground plane size suppresses the surface wave diffractions at the edges of the ground plane of the substrate of MI-OMSA which helps in improving in the radiation characteristics of the antenna structure. Also, the partial ground structure is useful in improving impedance bandwidth. As depicted in fig. 10, the antenna structure exhibits good reflection characteristics for the ground plane of size 3.5 mm × 37 mm than ground plane of size 40 mm × 37 mm.

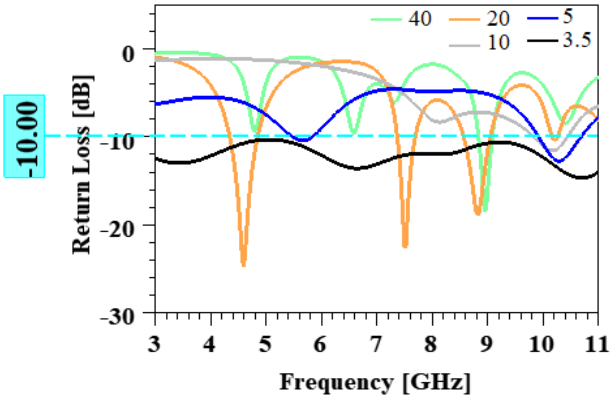


**FIGURE. 10:** Return Loss for different ground length dimensions (mm)

## B. EVALUATION FRAMEWORK

The simulated results of optimized HI-OMSA, VI-OMSA, MI-OMSA structures for return loss and VSWR are depicted in fig. 11 and fig. 12 respectively. The HI-OMSA structure provides two resonances at 3.75 and 8.2 GHz. The simulated $S_{11}$ values at these frequencies are -15.87 dB and -13.80 dB respectively resulting in poor performance due to less current distribution. The observed gain is 4.99 dB at frequency 8.2 GHz and 5.01 at the frequency 9.25 GHz then after increases linearly shown in fig. 13.

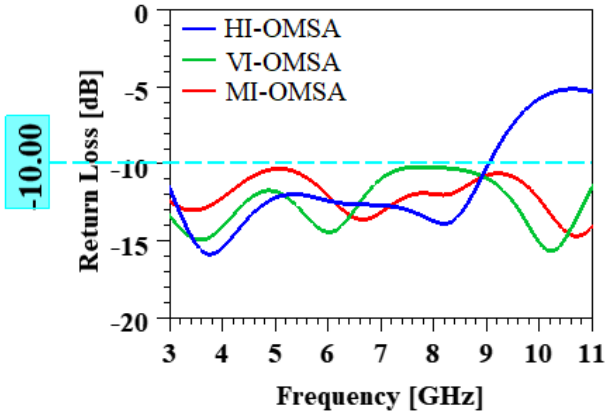


**FIGURE. 11:** Return Loss for different OMSA structures.

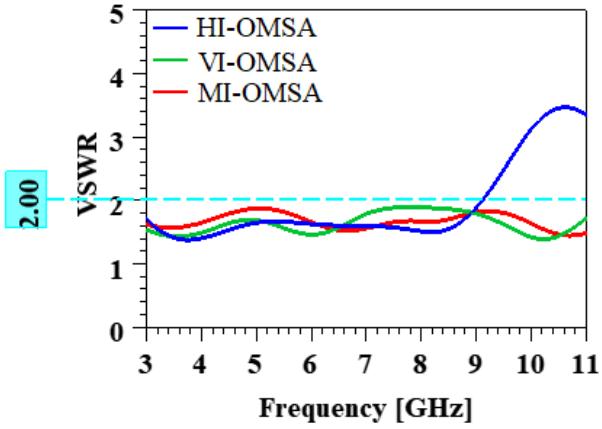


**FIGURE. 12:** VSWR for MI-OMSA structure.

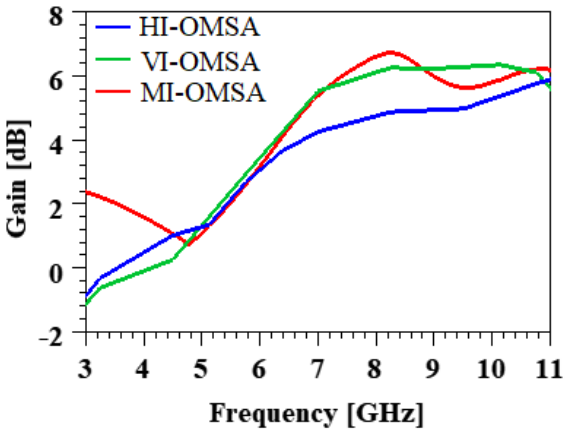


**FIGURE. 13:** Gain Variations for different OMSA structures.

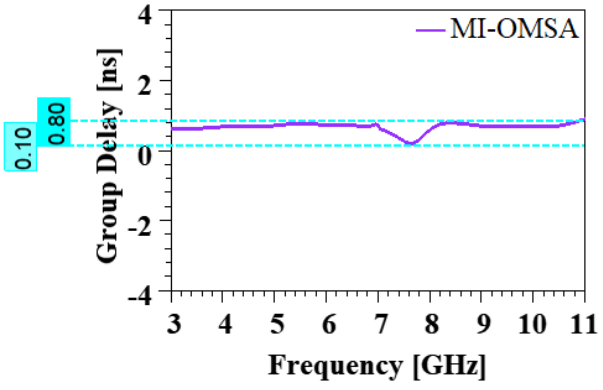


**FIGURE. 14:** Group Delay over UWB frequency range for MI-OMSA structure.

The vertically integrated structure is resonating at three different frequencies 3.54, 6.01, 10.2 GHz with $S_{11}$ values of -14.81, -14.33, -15.58 dB respectively providing bandwidth of 8.88 GHz from 2.37 to 11.25 GHz. The peak gain observed is near about 6.3 dB from 8.2 – 10 GHz. The negative gain is observed at the lower frequencies affecting antenna radiation performance. To boost gain at the lower frequencies small slot is etched off in the ground plane. Also, two slots of dimensions

2 mm × 2 mm are etched off the radiator helps to enhance the impedance bandwidth and contribute to boost small amount of gain. This modified integrated structure provides improvement in the gain of 0.4 dB and in the impedance bandwidth of 430 MHz. The simulated MI-OMSA is resonating at four different frequencies 3.45, 6.675, 8.2 and 10.67 GHz with S11 values of -12.97, -13.26, -12.02, -14.75 dB respectively and provides return loss less than -10 dB over 2.42 – 11.72 GHz frequency range, covering bandwidth of 9.31 GHz. The MI-OMSA fabricated structure is resonating at 3.15, 6.20, 10.2 GHz with $S_{11}$ values of -14.39, -14.15, -13.74 dB respectively. The observed peak gain value of simulated and measured structure is 6.734 and 6.635 dB at the frequency 8.2 GHz and 7.9 GHz respectively. The defective ground made by etching off the smaller slit S3 contributes in enhancing impedance bandwidth but results in a short fall of gain at 4.8 GHz. The MI-OMSA structure provides VSWR < 2. The low variations in group delay from 0.2 ns - 0.8 ns for 100 mm distance are observed ensuring almost constant group delay over the UWB spectrum. The simulated results for group delay are shown in fig 14. The radiation pattern, electric field distribution and current distribution are depicted in fig. 15, 16 and 17 respectively. The antenna structures offer radiation pattern of omnidirectional and hence are most fit for use in UWB applications. The deteriorated radiation patterns are observed at higher frequencies due to higher magnitudes observed at higher order modes and unalike phase distribution of electrical fields on the slot. The radiation pattern can be improved by increasing the slot dimensions.

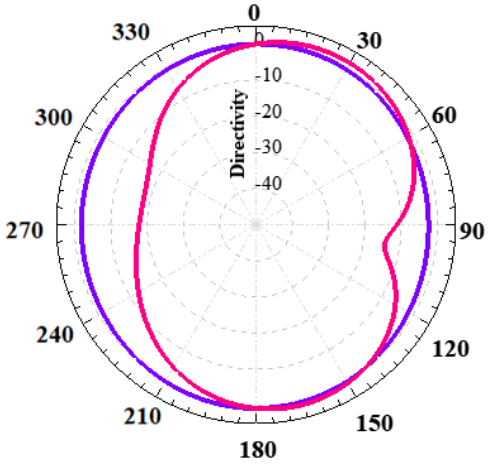


(i) Directivity ($E_\theta$) at 3.5 GHz

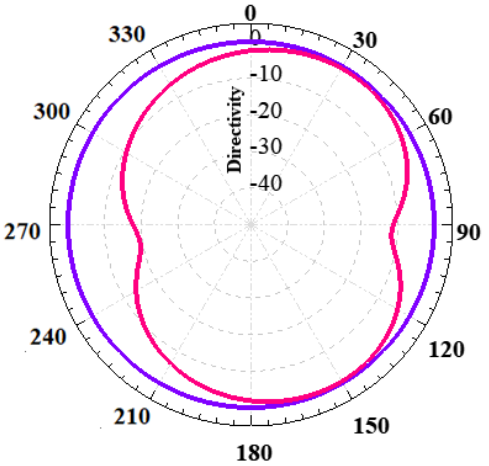


(ii) Directivity ($E_\phi$) at 3.5 GHz

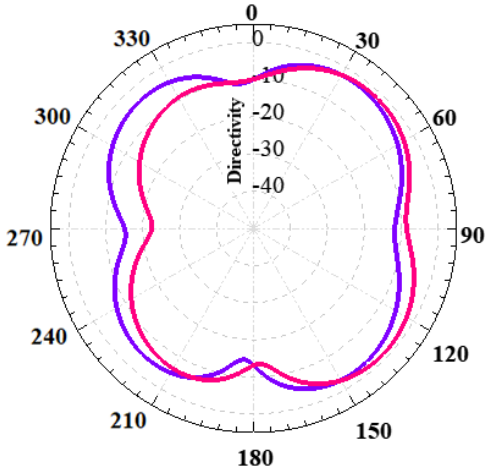


(iii) Directivity ($E_\theta$) at 6.6 GHz

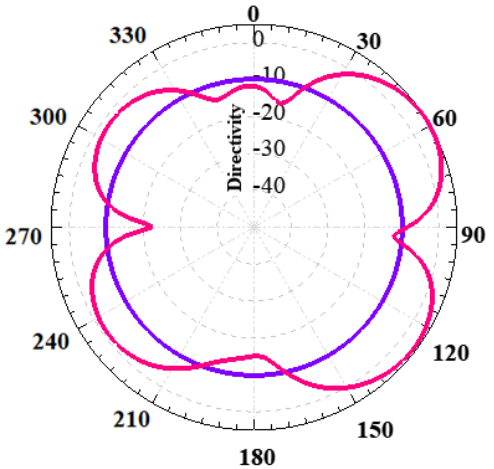


(iv) Directivity ($E_\phi$) at 6.6 GHz

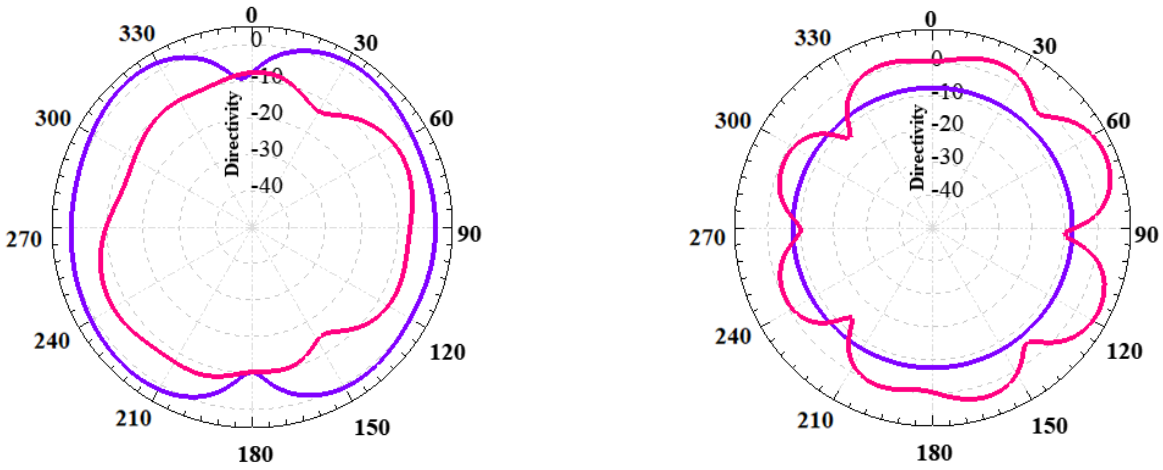


(v) Directivity ($E_\theta$) at 10.2 GHz (vi) Directivity ($E_\phi$) at 10.2 GHz

**FIGURE. 15:** Radiation pattern of Modified Octagonal MSA

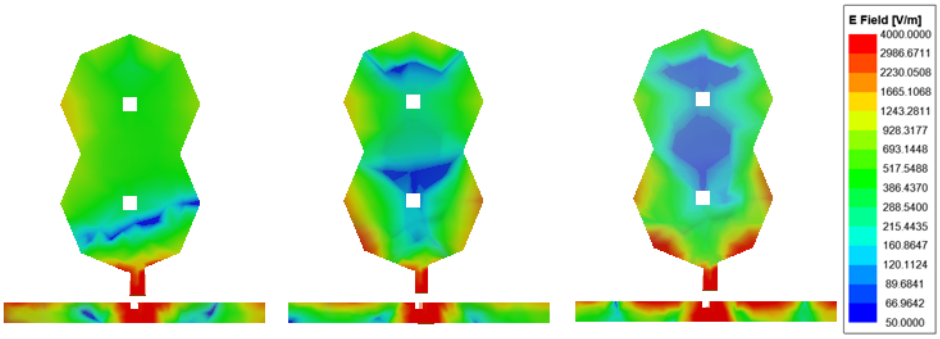


(i) 3.5 GHz (ii) 6.6 GHz (iii) 10.2 GHz

**FIGURE. 16:** Electric field Distribution of Modified Octagonal MSA

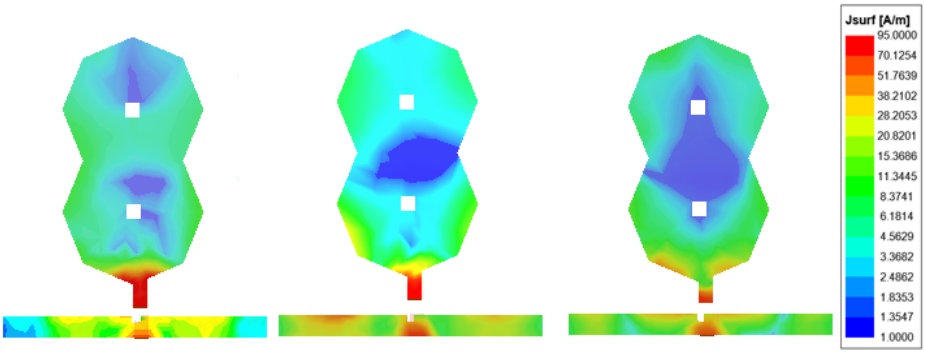


(i) 3.5 GHz (ii) 6.6 GHz (iii) 10.2 GHz

**FIGURE. 17:** Current Distribution of Modified Octagonal MSA

The MI-OMSA antenna structure is fabricated by using double sided copper flame retardant epoxy glass composite dielectric substrate. The substrate material used is of 1.6 mm thick, $\varepsilon_r$ of 4.4 and tan δ of 0.02. The fabricated antenna prototype of MI-OMSA is presented in fig. 18. The structure is tested and results are validated by using vector network analyzer model N9916A. The optimized results from the simulator and measured results from VNA of return loss and gain variations for both the structure are shown in fig. 19 and 20 respectively. An ultra-wideband performance is achieved as antenna resonates at different frequencies.

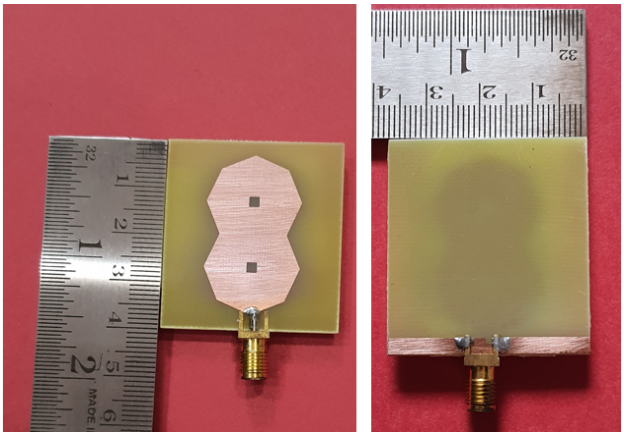

**FIGURE. 18:** Fabricated Modified Octagonal MSA (MI-OMSA) Structure

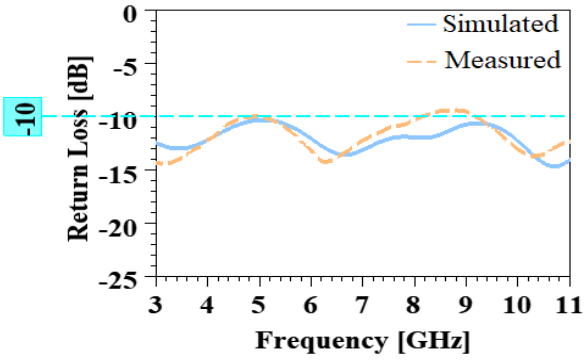


**FIGURE. 19:** Return Loss of S-OMSA and MI-OMSA

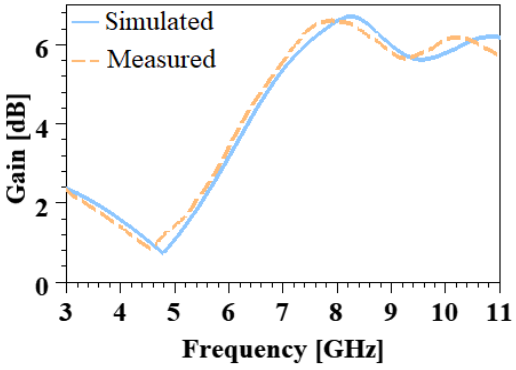


**FIGURE. 20:** Gain variations of MI-OMSA

### C. UWB APPLICATION: BREAST TUMOR DETECTION

The proposed octagonal microstrip antenna structure is used for UWB application; detection of the tumor presence in the breast. The entire system model is comprised of MI-OMSA antenna structure and breast phantom. Here, the breast phantom of diameter 45 mm is modelled by using HFSS software. The model is of heterogeneous type consisting four layers of the breast namely, skin, fat, fibro glandular and tumor. Figure 21 and 22 depicts the layered structure of the heterogeneous breast phantom, which is the most realistic form. The fatty and glandular layers comprise approximately 50% of the thickness, whereas the skin layer is pretty thin. The skin layer of 2 mm thick, the fatty layer of 18 mm thick, the glandular layer of 25 mm thick, and a 5 mm tumor has been embedded in the gland layer. Through these layers of the breast, the radiation from the antenna sensor will enter and interact with the breast tissues. Since breast tissues appear to be a lossy dispersive material for microwave propagation, the dispersive effect must be taken into account in order to deal with the actual electrical characteristics of the breast tissues. These biological components provide a signal as a result of microwave properties like as absorption, transmission, and reflections. The figure 23 demonstrates the reflection characteristics of the entire system model. When compared to a breast phantom without a tumor, the one with the tumor layer showed a significant change in reflection characteristics because the malignant tissues absorbed more radiation.

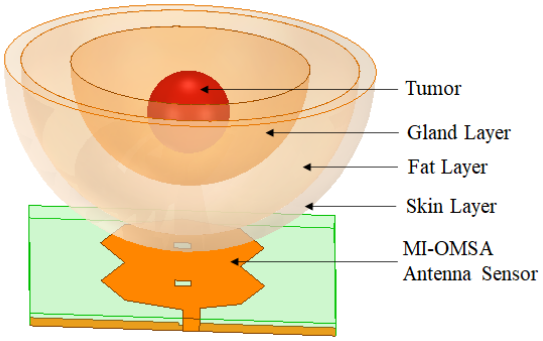


**FIGURE. 21:** MI-OMSA with Breast Phantom Model

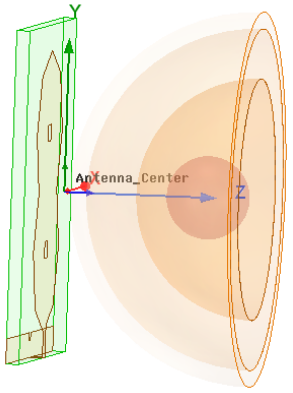


**FIGURE. 22:** Side view of MI-OMSA with Breast Phantom Model

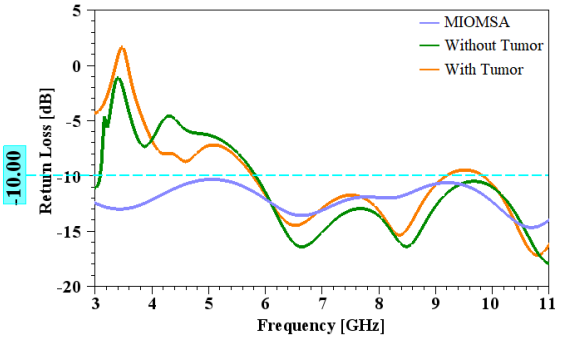


**FIGURE. 23:** Reflection Characteristics of MI-OMSA with Breast Phantom for Tumor of size 5 mm

## IV. COMPARISION WITH LITERATURE

The proposed modified integrated octagonal microstrip antenna (MI-OMSA) is designed to operate in ultra-wide band frequency spectrum and will be used to analyze the dielectric properties of the different layers of the breast phantom. Hence the antenna structure is compared with the UWB antennas used for the application of breast tumor detection in the literature with respect to antenna size, dielectric properties, operating frequency spectrum and gain.

**TABLE II.** Comparison of invented UWB antennas with proposed antenna.

| Ref. No. | Antenna Configuration | Antenna Size (mm × mm) | Substrate Used | Dielectric Properties | | Band (GHz) | Gain (dB) |
|---|---|---|---|---|---|---|---|
| | | | | Permittivity | Thickness (mm) | | |
| [4] | Hexagonal Monopole antenna with asymmetrical U-slot for UWB applications | 30 × 30 | RT5880 | 2.2 | 1.57 | 4-14 | 2.2 - 3.6 |
| [5] | MS-fed Circular radiator with open T-slot in ground plane for portable UWB applications | 30 × 35 | FR4 | 4.4 | 0.8 | 2.5-12.5 | 4.1 |
| [8] | Proximity feed, open ring slot circular patch with π-shaped slot in feedline with two band rejections. | 20 × 25 | FR4 | 4.7 | 1.5 | 2.7-17 | 4.5 |
| [9] | Octagonal MSA with circular slot by tapered strip line fed and elliptic geometry slot at ground with reduced RCS for UWB applications. | 70 × 60 | Arlon Diclad 880 | 2.2 | 0.762 | 2.5-18 | 3.8 |
| [10] | MS fed dodecagon shaped monopole antenna operating in UWB for breast cancer detection. | 40 × 38 | FR4 | 4.4 | 1.6 | 3-17 | 5 |
| [11] | Square monopole antenna with two rectangular ring self-complementary structure to enhance the bandwidth for microwave imaging applications. | 14 × 22 | FR4 | 4.4 | 0.8 | 3.04-11.43 | 3-5 |
| [13] | Offset MS fed square ring shape UWB antenna with slotted partial ground for breast tumor detection. | 20 × 35 | FR4 | 4.4 | 1.6 | 2.9-13 | 5.2 |
| [14] | I-shaped rectangular MSA with two rectangular parasitic elements for imaging systems to detect breast cancer. | 40 ×30 | FR4 | 4.4 | 3 | 4.9-7.89 | 2.45 |
| [15] | Planar rectangular slotted radiator with tapered slot ground for microwave imaging-based breast tumor detection | 21.44 × 23.53 | FR4 | 4.4 | Not Reported | 3.49-12 | 5.76 |
| [16] | Rectangular UWB antenna for breast microwave radar-based imaging to detect tumor. | 20.5 × 10.6 | FR4 | 4.7 | 1.6 | 3-18 | 4.41 |
| [17] | Four element elliptical shaped MIMO antenna by with stubs on either side of ground to provide high isolation for breast cancer detection. | 71.5 × 16 | Rogers RT/Duroid 5880 | 2.4 | 0.254 | 3.2-14 | 5.6 |
| [18] | Octagonal ring shaped UWB antenna with parasitic resonator for microwave imaging applications | 24 × 29 | FR4 | 4.3 | 1.5 | 2.8-11.5 | 5.8 |
| [19] | MS fed modified rectangular MSA with circular resonator base antenna for breast cancer detection. | 20 × 30 | FR4 | 4.4 | 1.6 | 3.1-6.8 | 4.8 |
| [20] | Planar circular slotted radiator with rectangular defected ground structure for microwave breast imaging. | 18 × 28 | FR4 | 4.3 | 1.6 | 3.4-10 | 3.95 |
| [21] | CPW fed elliptical shaped MSA with two inverted U-slots for on-body application. | 30 × 24 | FR4 | 4.4 | 1.5 | 3-10.7 | -1.98 |
| [22] | Inverted L-shaped monopole antenna with semi-circular section and parasitic element for tri-band operation. | 32 × 21 | FR4 | 4.4 | 1.6 | 2.1-2.485<br>5.05-5.67<br>8.4-9 | 3.8 |
| PA (MI-OMSA) | Integrated octagonal radiator with rectangular slot and slit in ground plane for UWB application. | 37 × 40 | FR4 | 4.4 | 1.59 | 2.42-11.72 | 6.7 |

## V. CONCLUSION

An integrated-octagonal radiating patch configuration for gain enhancement is presented. The proposed antenna structure is optimized by using high-frequency structure simulator 2022 R2 software, developed on double sided copper FR4 epoxy glass substrate and tested using vector network analyzer model N9916A. The gain enhancement is obtained by integrated patch configuration. The modified integrated prototype is fabricated on double sided copper flame retardant 4 epoxy glass substrate of size 37 mm × 40 mm and tested using vector network analyzer. The MI-OMSA provides bandwidth of 9.31 GHz from 2.42 - 11.72 GHz. The peak gain observed at frequency 8.2 GHz is 6.7 dB. The constant group delay less than 0.8 ns is observed over the operating spectrum. The designed MI-OMSA offers quad tuned ultra-wideband behavior as it resonates at 3.45, 6.675, 8.2 and 10.2 GHz frequencies below -10 dB of reflection coefficient values. The multiple resonance frequencies are useful in deeper penetration of an object. The proposed antenna is simulated with breast phantom of 45 mm diameter, providing multiple resonance. The developed antenna structures provide higher bandwidth and sufficient gain making better fit to analyze dielectric properties of different layers of the breast. Hence developed antenna structures are most suitable for breast tumor detection.

## REFERENCES


[1] Federal Communication Commission, “First report and order, revision of part 15 of the commissions rule regarding ultra-wideband transmission systems”, Technical report, Washington, DC, Apr. 2002.

[2] Ray, K. P., “Design aspects of printed monopole antennas for ultra-wide band applications”, International Journal of Antennas and Propagation, Vol. 2008, 1–8, 2008.

[3] Dastranj A., A. Imani, and M. Naser-Moghaddasi, “Printed wide-slot antenna for wideband applications”, IEEE Transactions on Antennas and Propagation, Vol. 56, No. 10, 3097–3102, Oct. 2008.

[4] Abdo Abdel Monem Shaalan & M. I. Ramadan, “Design of a Compact Hexagonal Monopole Antenna for Ultra-Wideband Applications", J Infrared Milli Terahz Waves, 31:958–968, 2010, doi: 10.1007/s10762-010-9654-8.

[5] X. F. Zhu and D. L. Su, “A Study of a Compact Microstrip-Fed UWB Antenna with an open T-Slot", Progress in Electromagnetics Research M, Vol. 13, 181-189, 2010.

[6] Sanjeev K. Mishra, Rajiv K. Gupta and Jayanta Mukherjee, “Effect of Substrate Material on Radiation Characteristics of an UWB Antenna”, Antennas & Propagation Conference Loughborough, UK, 2010

[7] Chia Ping Lee, Chandan Kumar Chakrabarty, “Ultra Wideband Microstrip Diamond Slotted Patch Antenna with Enhanced Bandwidth”, International Journal Communications, Network and System Sciences, 4, 468-474, doi:10.4236/ijcns.2011.47057, 2011.

[8] Mohamed Mamdouh M. Ali1, Ayman Ayd R. Saad and Elsayed Esam M. Khaled, “A Design of Miniaturized Ultra-Wideband Printed Slot Antenna With 3.5/5.5 GHz Dual Band-Notched Characteristics: Analysis and Implementation", Progress in Electromagnetics Research M, Vol. 52, 37-56, 2013.

[9] Dikmen Cengizhan M., Cimen Sibel and Cakir Gonca, “Planar Octagonal-Shaped UWB Antenna with Reduced Radar Cross Section”, IEEE Transactions on Antennas and Propagation, 62(6), 2946–2953, doi: 10.1109/TAP.2014.2313855, 2014.

[10] Kahar, M., A. Ray, D. Sarkar, and P. P. Sarkar, “An UWB microstrip monopole antenna for breast tumor detection”, Microwave and Optical Technology Letters, Vol. 57, No. 1, 49–54, 2015.

[11] Ojaroudi, Mohammad and Ozlem Aydin Civi, “Bandwidth enhancement of small square monopole antenna using self-complementary structure for microwave imaging system applications”, The Applied Computational Electromagnetics Society Journal, 1360-1365, 2015.

[12] Amal Afyf, Larbi Bellarbi, Anouar Achour, Fatima Riouch, Abdelhamid Errachid, “A Novel Low Cost UWB Antenna for Early Breast Cancer Detection”, American Journal of Electromagnetics and Applications, ISSN: 2376-5968 (Print); ISSN: 2376-5984 (Online), doi: 10.11648/j.ajea.20150305.11, 2015.

[13] Ibtisam Amdaouch, Otman Aghzout, Azzeddin Naghar, Ana V. Alejos, and Francisco Falcone, “Breast Tumor Detection System Based on a Compact UWB Antenna Design", Progress in Electromagnetics Research M, Vol. 64, 123-133, 2018.

[14] T. V. Padmavathy, P. Venkatesh, D. Bhargava, N. Sivakumar, “Design of I-shaped dual C-slotted rectangular microstrip patch antenna (I-DCSRMPA) for breast cancer tumor detection", Cluster Computing, Springer, doi:10.1007/s10586-018-2161-8, 2018.

[15] Islam Md Tarikul, M. Samsuzzaman, M. Faruque, Mandeep Jit Singh, and M. Islam, “Microwave imaging-based breast tumor detection using compact wide slotted UWB patch antenna”, Optoelectronics and Advanced Materials - Rapid Communications, Vol. 13., No 7-9, 448-457, 2019.

[16] Avsar Aydin, E., Kaya Keles, M., “UWB Rectangular Microstrip Patch Antenna Design in Matching Liquid and Evaluating the Classification Accuracy in Data Mining Using Random Forest Algorithm for Breast Cancer Detection with Microwave", Journal of Electrical Engineering and Technology, Springer, 2019, doi:10.1007/s42835-019-00205-x.

[17] Rao, P. K. and R. Mishra, “Elliptical shape flexible MIMO antenna with high isolation for breast cancer detection application,” IETE Journal of Research, 1–9, 2020.

[18] Hossain Amran, Islam Mohammad Tariqul, Almutairi Ali F., Singh Mandeep Singh Jit, Mat Kamarulzaman, Samsuzzaman Md., “An Octagonal Ring-shaped Parasitic Resonator Based Compact Ultrawideband Antenna for Microwave Imaging Applications”, Sensors, 20(5), 1354, March 2020, doi:10.3390/s20051354.

[19] Praveen K. Rao and Rajan Mishra, “Resonator Based Antenna Sensor for Breast Cancer Detection", Progress in Electromagnetics Research M, Vol. 101, 149-159, 2021.

[20] Venkata L. N. Phani Ponnapalli, Shanumugam Karthikeyan, and Jammula L. Narayana, “A Circular Slotted Shaped UWB Monopole Antenna for Breast Cancer Detection", Progress in Electromagnetics Research Letters, Vol. 104, 57-65, 2022.

[21] Sri Pasumarthi Amala Vijaya, and Ketavath Kumar Naik, “U-Slotted Elliptical Shape Patch Antenna for UWB On-Body Communications”, Progress in Electromagnetics Research Letters 104, 77-85, 2022

[22] Khade Alka, Mahadu Annarao Trimukhe, Shishir Jagtap, and Rajiv Kumar Gupta, “A Circular Sector with an Inverted L Shaped Monopole Antenna for Tri-Band Applications”, Progress in Electromagnetics Research C 118, 177-186, 2022.

[23] Mezaal Yaqeen S., Kadhum Al-Majdi, Aqeel Al-Hilalli, Alabbas A. Al-Azzawi and Aya A. Almukhtar, “New miniature microstrip antenna for UWB wireless communications”, Proceedings of the Estonian Academy of Sciences 71, no. 2, 194-202, 2022.

[24] Celik Kayhan, Hasan Huseyin AK, and Erol Kurt, “Design and Analyses of the Novel Circular Fractal UWB Antenna”, European Conference on Renewable Energy Systems Istanbul/Turkey 07-09 May 2022.

[25] K. C. Gupta, R. Garg, I. Bahl and P. Bhartia, “Microstrip Lines and Slotlines,” 2nd Edition, Artech House, Boston London, 1996.

[26] Ibtisam Amdaouch, Otman Aghzout, Azzeddin Naghar, Ana Vazquez Alejos, Francisco Falcone, “Design of UWB Compact Slotted Monopole Antenna for Breast Cancer Detection”, Advanced Electromagnetic, Vol-8 No. 5., 2019

[27] Sara Yehia Abdel Fatah, Fatma Taher, Taha Elwi, Mohamed Fathy Abo Sree, Mohammad Alibakhshikenari, Bal Virdee, Patrizia Livreri, Naser Ojaroudi Parchin, Chan Hwang See, Giovanni Pau, Iyad Dayoub, Ernesto Limiti, ‘Design of Compact Flexible UWB Antenna

Using Different Substrate Materials for WBAN Applications', Photonics & amp; Electromagnetics Research Symposium (PIERS), Prague, Czech Republic. pp.373-378, 2023. doi: 10.1109/PIERS59004.2023.10221357

[28] Kamil Karaçuha, Feza Turgay Çelik, and Halil Ismail Helvaci, "A Multi-Mode Pattern Diverse Microstrip Patch Antenna Having a Constant Gain in the Elevation Plane", Advanced Electromagnetic, Vol-12 No.-4, 2023.

[29] Taha A. Elwi1, Areeg A. M. Al-Shaikhli Hayder H. Al-Khaylani, and Rusul Khalid Abdulsattar, "Reconfigurable Metamaterial Antenna based an Electromagnetic Ground Plane Defects for Modern Wireless Communication Devices", Advanced Electromagnetic, Vol-3 No.-1, 2024.